conf-405-32 (1,d)

MASTER

LAVES PHASES OF THE RARE EARTHS WITH TRANSITION ELEMENTS

Rodney P. Elliott
IIT Research Institute, Chicago, Illinois, 60616

Facsimile Price $ 3.60
Microfilm Price $ 1.16

Available from the
Office of Technical Services
Department of Commerce
Washington 25, D. C.

DISCLAIMER

LAVES PHASES OF THE RARE EARTHS WITH TRANSITION ELEMENTS

ABSTRACT

The alloying characteristics of the rare earth elements with the transition metals undergo a radical change as the atomic number of the transition series increases--transition elements in Groups IVa, Va, and VIa are immiscible with the rare earths, while elements of Groups VIIa, and VIIIa, VIIIb and VIIIc form many compounds. Since this cannot be correlated with a size effect, a reasonable explanation for this behavior is a valency or electronegativity effect. Those binary systems forming compounds form "Laves phases," which can exist in one of three related crystal structure types: $MgCu_2$, $MgZn_2$, or $MgNi_2$. The specific Laves-type crystal structure can be related to the average free electron concentration, a phenomenon which has been used to calculate electronic valency of the transition elements. A compilation of the known Laves-type phases occurring between rare earth elements and transition metals supports the hypothesis that the valency effect is operative. Additional rare earth-transition metal compounds previously unknown have been prepared and found to be consistent with the previously noted trend.

On the assumption that a critical electron/atom ratio determines which Laves-type structures are stable, the periodical grouping of the Laves-type species of the rare earth-transition metal compounds indicates a slight but regular increase in valency as the atomic number of the rare earth increases. Ternary alloys prepared between the Laves phases of different structure types substantiate the observed valency trend.

LAVES PHASES OF THE RARE EARTHS WITH TRANSITION ELEMENTS

I. INTRODUCTION

Although the rare earth elements are chemically very similar, they present a dichotomy with respect to alloying behavior with the transition elements. Known binary systems with Groups IVa, Va, and VIa elements form no compounds, the systems often displaying immiscibility in the liquid as well as the solid state. Alloys with the Group VIIa, VIIIa, VIIIb, and VIIIc elements form numerous intermetallic compounds. This complete change in alloying behavior apparently is not related to the size factor phenomenon, but to valency or electronegativity effects.

Because of the basic similarity of the properties of the rare earths, a unique group of elements is available for alloy theory studies. Since the rare earth elements are transition elements, the results of such studies are immediately applicable to that group of metals from which most of the modern alloys are fabricated.

The analysis of alloy formation was first discussed by Hume-Rothery, who found that certain compounds of known crystal symmetry could be rationalized in terms of their electron/atom ratio using the common valences associated with chemical compounds. These compounds have subsequently been termed "Hume-Rothery compounds." Attempts to analyze solid solution formation and intermetallic compound formation of less noble metal systems using the concepts of Hume-Rothery have been less successful. This is understandable since the Hume-Rothery compounds are metallic and stability is governed by free electron effects rather than by ionic characteristics.

Specific types of intermetallic compounds are known to occur in binary systems having similar metallurgical properties. In most instances such occurrences do not permit detailed calculations to be made with regard to their specific alloying characteristics. A notable exception to this, however, is the Laves phases--i. e., intermetallic compounds having crystal structures isotypic with $MgCu_2$, $MgZn_2$, and $MgNi_2$.

There is a marked similarity among the crystal lattices of the three Laves-type compounds. For the AB_2 prototype compounds, with respect to the A atom, $MgCu_2$ consists of double layers of hexagonal arrays of A atoms stacked abcabc; $MgZn_2$ consists of double layers of A atoms stacked ababab; and $MgNi_2$ consists of double layers of A atoms stacked abacabac. The B atoms surround the A atoms in tetrahedra. The manner in which these tetrahedra are connected is dependent on the particular crystal type.

The existence of Laves phases is governed primarily by space-filling considerations. For these structures the theoretical atomic diameter ratio is 1.225; however, Laves phases are known for the d_A/d_B spectrum from 1.05 to 1.68, although the great majority occur between 1.12 to 1.38.* It has been adequately demonstrated by Dwight (1) that there is no correlation between the Laves phase structure type and the atomic diameter ratio.

Electronic factors have been shown to be operative governing which crystal type is stable. In a series of projects over a 3 1/2 year period at IIT Research Institute (2-4) it has been demonstrated that for a

---

* For discussion of the theoretical atomic diameter ratio and the description of the crystal structures, the reader is referred to standard texts

common A element the structure type goes through the sequence $MgCu_2$ —> $MgZn_2$ —> $MgCu_2$ as the B element increases in atomic number for a given period. Examples of this behavior are shown for zirconium, columbium, and hafnium with elements of the first transition series in Figure 1. The full sequence is not observed for A elements titanium and tantalum, because the size factor becomes conducive to continuous or extended solid solutions. The non-occurrence of Laves phases for binary systems of transition elements with nickel is not satisfactorily explained but is probably due to electronic considerations.

Binary Laves phases alloy readily with each other. Ternary alloys between binary compounds of different crystal structure show but a narrow composition region that is two-phase. Ternary alloys between $MgCu_2$ structures at the extremes of the sequence show an intermediate compositional region in which alloys have the $MgZn_2$ structure. The latter phenomenon is further substantiation of the dependence of the crystal structure of Laves phases on electronic rather than on the atomic diameter ratio. From such it may also be concluded that the electron valency of elements for a given transition series varies monotonically with the atomic number. Witte (5) has calculated electron/atom volumes of Brillouin zones for Laves phase compounds and shows tangencies of the Fermi sphere for the $MgCu_2$ structure at an electron/atom ratio of 1.83, and 1.93 and 2.32 for the $MgZn_2$ structure. The value 1.83 is consistent with 1.80 observed experimentally by Laves and Witte (6) by diluting the prototype phases with aluminum, zinc, silver, silicon and using the common metallic valencies in the calculations. Elliott and Rostoker (4) have applied the electron/atom ratios of 1.80 and 2.32 to calculate a consistent set of valencies for the transition elements assuming 4 for titanium. Further work by Elliott (3) showed that it is impossible to use such methods for calculating a complete set of consistent valencies since other variables affect the composition limits.

Laves-type phases occur regularly in alloys of the rare earth metals with the transition metals. Dwight (1) has inferred that the sequence $MgCu_2$ —> $MgZn_2$ —> $MgCu_2$ is likewise operative for rare-earth base Laves-type phases. As yet, however, the complete sequence has not been observed experimentally. The present investigation was undertaken with two objects in mind: (a) to prepare binary Laves phases between the rare earth elements and the transition metals so that the $MgCu_2$ —> $MgZn_2$ —> $MgCu_2$ sequence could be more precisely positioned as to its dependence on the periodic table (and hence valency), and (b) to prepare ternary Laves phases between these binary compounds to ascertain the relative valencies of the rare earth elements on the assumption the $MgCu_2$ —> $MgZn_2$ —> $MgCu_2$ transitions occur at known electron/atom ratios.

II. EXPERIMENTAL TECHNIQUES

Materials of highest available purity were obtained for the production of alloys.

Wherever feasible, nonconsumable arc melting techniques were used in preparing the alloy compositions. The form of the as-received material dictated, in part, the melting technique. Many of the rare earths were available as sponge, which is powdery. Sponge and transition metal powders were blended and compacted prior to arc melting. Powder was prepared by filing those transition metals not available as powder. If the rare earth was available as solid material, the arc-melting technique used was to place the higher melting constituent on top before melting. Because of the expensive nature of the component materials, small ingots weighing 3 grams were produced. Ingots were remelted several times to insure homogeneity of composition. After melting, the ingots were annealed 16 hours at 1000°C in argon to eliminate any microinhomogeneities resulting from peritectic formation of intermetallic compounds.

The wide divergence of the melting points of the component elements made arc-melting techniques unsuitable in many instances. Electron beam melting, levitation melting, and very high pressure sintering were attempted unsuccessfully, the latter because of temperature limitations of equipment. Liquid-phase sintering in columbium crucibles was effective for alloys containing osmium, ruthenium, or rhenium. In these instances the rare earth metal was pickled, the alloy charge weighed, and the columbium crucible welded closed in a helium atmosphere. Alloys prepared by liquid-phase sintering were, in general, not as homogeneous as those prepared by arc-melting.

Annealed specimens were prepared for diffraction studies by crushing in a steel mortar. Powder of -200 mesh was used. Powder patterns were indexed by Hull-Davey charts. Accurate lattice parameters were obtained by a least-squares IBM 7090 program in which the systematic absorption error proportional to the trigonometric Nelson-Riley function was incorporated.

III. EXPERIMENTAL RESULTS

The results of X-ray investigations of binary AB_2 compositions are summarized in Tables 1 and 2. These data, together with the previously known data for Laves-type compounds, are shown graphically with respect to the periodic table in Figures 3, 4, and 5.

The results of the X-ray investigation of ternary alloys of AB_2 composition are summarized in Table 3 and shown graphically in Figures 6, 7, and 8. The dots in these figures indicate those compositions actually prepared.

IV. DISCUSSION

A. Binary Laves Phases

As is evident in Figures 3, 4, and 5, the structure type of known Laves phases is distributed regularly as a function of the periodic table. The only exception to this is $NdMn_2$ which was both found and verified to have the $MgZn_2$ structure in a field where the $MgCu_2$ structure is more probable. From a scrutiny of distribution of the $MgCu_2$ and $MgZn_2$ structures, several important conclusions are made:

1. Laves-type phases exist with regularity with all rare earth elements for the transition elements in Groups VIIa, VIIIa, VIIIb, and VIIIc. Since the d_A/d_B ratio is favorable for all combinations, the nonexistence of Laves-type phases must be attributed to either (a) electronic considerations--that is, an unfavorable electron/atom ratio--or (b) free energy or electronegativity restrictions imposed by the system.

2. While the great majority of rare earth Laves phases are of the $MgCu_2$ type, the existence of the $MgZn_2$ type of structure occurs in such a pattern to indicate that the transition $MgCu_2 \longrightarrow MgZn_2 \longrightarrow MgCu_2$ exists. Thus the electronic valency governs which type of structure is stable. The complete $MgCu_2 \longrightarrow MgZn_2 \longrightarrow MgCu_2$ transition, however, is in no instance observed.

3. For a given transition element period there is the tendency for the $MgZn_2 \longrightarrow MgCu_2$ discontinuity to move to the right (that is, to higher atomic number) as the rare earth A element increases in atomic number. On the assumption that the electron valency decreases as the atomic number of the transition element period increases, the discontinuity shift suggests that there is a slight but regular increase in valency as the atomic number of the rare earth increases.

4. In comparison of the three transition series, the discontinuity between the $MgZn_2$ and the $MgCu_2$ types shifts from left to right in going from the first to the second transition series, and from rare earths of high atomic number to low atomic number in going from the second transition series to the third transition series. Such shifts suggest a net increase in valency for a given periodic group in successive periods (e.g., $v_{Fe} < v_{Ru} < v_{Os}$).

B. Ternary Alloys

The periodic variation of structure type was indicative of the controlling factor of the free electron concentration. Ternary alloys were necessary to amplify the binary findings so that quantitative calculations could be made. Ternary alloys were made on the basis of the binaries to provide information regarding (a) the relative valencies for the rare earths, (b) the reasons for the non-occurrence of the complete $MgCu_2$ —> $MgZn_2$ —> $MgCu_2$ trend, and (c) the reasons for the non-existence of Laves phases, or indeed, compounds for the rare earths with transition metals of groups IVa, Va, or VIa.

The valencies of the rare earth metals may be calculated from the miscibility between the binary Laves phases in Figure 6a-6f, and Figure 7d-7e. The basis of the calculations are (a) that the $MgCu_2$-structure miscibility limit is electron dependent and exists at the electron/atom ratio of 1.80 as given by Witte (5), and (b) that the free electron valancies of the transition metals calculated by Elliott and Rostoker (3) on this assumption are applicable--namely $v_{Ti} = 3.92$, $v_V = 2.19$, $v_{Cr} = 1.69$, $v_{Mn} = 1.35$, $v_{Fe} = 0.92$, $v_{Co} = 0.72$, and $v_{Ni} = 0.25$.

From Figure 7, d and e, the limits of the $MgCu_2$ miscibility are taken as 25 a/o $ErMn_2$ for the $Er(Mn + Fe)_2$ ternary, and 35 a/o $ErMn_2$ for the $Tm(Mn + Fe)_2$ ternary. Therefore,

$$V_{Er} + 2(0.75\ v_{Mn} + 0.25\ v_{Fe}) = 3 \times 1.80$$

$$V_{Er} + 2(0.75 \times 1.35 + 0.25 \times 0.92) = 3 \times 1.80$$

$$v_{Er} = 2.92 \text{ electrons/atom}$$

and,

$$V_{Tm} + 2(0.65\ v_{Mn} + 0.35\ v_{Fe}) = 3 \times 1.80$$

$$V_{Tm} + 2(0.65 \times 1.35 + 0.35 \times 0.92) = 3 \times 1.80$$

$$V_{Tm} = 3.00 \text{ electrons/atom}$$

It is therefore quite apparent that the accuracy with which the valencies may be calculated is very dependent upon the accuracy with which the limit of the $MgCu_2$ miscibility range may be defined. The accuracy of v_{Er} is thus more precisely defined than v_{Tm} by the above calculations.

From the calculated value of v_{Er}, the values of v_{Sm}, v_{Gd}, v_{Dy}, and v_{Ho} may be calculated from the miscibility ranges shown in Figures 6a-6d. For example,

$$0.55\ v_{Dy} + 0.45\ v_{Er} + 2\ v_{Mn} = 3 \times 1.80$$

$$0.55\ v_{Dy} + 0.45 \times 2.92 + 2 \times 1.35 = 3 \times 1.80$$

$$v_{Dy} = 2.53 \text{ electrons/atom}$$

Similarly, $v_{Sm} = 2.04$, $v_{Gd} = 2.29$, and $v_{Ho} = 2.68$ electrons/atom.

The limit of the $MgCu_2$ miscibility may be calculated for the ternary system $(Dy + Tm)Mn_2$ in Figure 6e using these valencies. Assuming M to be the mol fraction of $TmMn_2$

$$M \times v_{Tm} + (1 - M)\ v_{Dy} + 2 \times v_m = 3 \times 1.80$$

$$M \times 3.00 + (1 - M)\ 2.53 + 2 \times 1.35 = 3 \times 1.80$$

$$M = 0.36, \quad 36 \text{ a/o } TmMn_2$$

in very good agreement with the experimentally observed limit of miscibility.

The free electron valencies calculated lie on a smooth curve increasing as the atomic number of the rare earth element increases, Figure 9. The extension of this curve indicates that the free electron valencies varies from ~1.5 electrons/atom for lanthanum to ~3.4 electrons/atom for lutetium.

The calculated limit of the $MgCu_2$ structure for the $(Ho + Tm)Mn_2$ system is 6 a/o $TmMn_2$. The experimentally observed limit (Figure 6e) is >10 a/o $TmMn_2$. The inconsistency of this system with the others is readily discernible by comparing it with the $(Ho + Er)Mn_2$ system. Since thulium has a higher valency than does erbium, less dilution of $HoMn_2$ with thulium than erbium should be required to bring the electron/atom ratio to a value greater than 1.80.

From Figure 9, approximate valencies of 1.5 for lanthanum, 1.8 for neodymium, and 1.6 for cerium may be taken. Thus, from the ternary $(La + Nd)Os_2$ (Figure 8a), a valency of ~1.90 for Os is calculable. The limit of the $MgCu_2$ structure miscibility in the $(La + Gd)Os_2$ and $(Ce + Gd)Os_2$ ternaries may then be calculated as 12 a/o $GdOs_2$ and 0 a/o $GdOs_2$, respectively. The former is in only approximate agreement with the experimental data given in Figure 8b. $MgCu_2$-type $CeOs_2$ apparently is stable at the critical electron/atom ratio of 1.80 consistent with the experimental data in Figure 8c.

If from Figure 8d the limit of the stability of $MgCu_2$ structure type is taken as 15 a/o $GdRu_2$, a free electron valency of 1.66 is calculated for ruthenium. Thus for the elements of Group VIIIa, $v_{Fe} < v_{Ru} < v_{Os}$ $(0.92 < 1.66 < 1.90)$, as had been predicted on the basis of the binary alloys.

Calculated valencies of the rare earth elements discussed to this point are consistent within themselves and with the previously calculated valencies of the transition elements. There are several areas where the valencies as calculated or the electronic theory present ambiguities.

1. On the basis of the previously accepted valency of chromium, and using the calculated valencies of the rare earth elements, the electron/atom ratio of all the binary systems of rare earths with chromium are favorable for the existence of Laves phases. It had been previously established that the size factor was satisfactory.

2. The non-existence of Laves phases of the transition elements with nickel had been interpreted by Elliott and Rostoker (3) to result from an electron/atom ratio below a minimum value, taken as ~1.3. Electron/atom ratios of all the rare earths with nickel are less than 1.3, yet all form Laves phases with nickel.

3. Dilution of the $MgZn_2$-type Laves phases with chromium should cause the electron/atom ratio to increase. At the value 2.32 the structure should revert to the $MgCu_2$ structure. Such does not occur. $ErMn_2$, $TmMn_2$, and $LuMn_2$ when diluted with chromium (Figure 7a-7c) generate the three-phase field of the $MgZn_2$ structure, rare earth, and chromium. The electron/atom ratio of the limit of the $MgZn_2$ structure type is ~2, much less than the assumed value of 2.32 for the condition of Fermi sphere tangency.

V. SUMMARY

On the basis of binary and ternary alloys of the $MgCu_2$ and $MgZn_2$ structure formed between the rare earth elements and the transition metals, a study of the free electron valency of the rare earth metals has been made. It is found that there is an increase in the valency as the atomic number of the rare earth metal increases. The calculated valencies increase from an estimated value of 1.5 electrons/atom for lanthanum to 3.4 electrons/atom for lutetium.

Experimental data are consistent for ternary systems in which the component binaries have Laves-type phases. The valencies calculated, however, do not permit explanation of the general theory of alloying of rare earth-transition metal systems. Stability of Laves-type phases for rare earth-chromium systems is predicted but not observed. Similarly, theory indicates the non-existence of Laves phases between the rare earth metals and nickel; Laves-type phases exist in all instances.

VI. ACKNOWLEDGEMENTS

The United States Atomic Energy Commission supported the investigations described in this paper on Contract No. AT(11-1)-578, Project Agreement No. 19. The author expresses his appreciation for the financial support.

Mr. Ronald Wibel did much of the routine alloy preparation and reading of the X-ray diffraction patterns.

REFERENCES

1. Dwight, A. E., Trans. ASM, 53, 479-500 (1961).
2. Elliott, R. P., Reports on Air Force Office of Scientific Research, Solid State Sciences Division, Contract Nos. AF 18(600)-642, AF 18(600)-1399, and AF 18(603)-130.
3. Elliott, R. P. and Rostoker, W., Trans. ASM, 50, 617-633 (1958).
4. Elliott, R. P., Trans. ASM, 53, 321-329 (1961).
5. Witte, H., "Zur Struktur und Materie der Festkörper," pp. 272-304 (1952), Springer, Berlin.
6. Laves, F. and Witte, H., Metallwirtschaft, 15, 840 (1936).
7. Baenziger, N. C. and Moriarty, J. L., Jr., Acta Cryst., 14, 948-949 (1961).
8. Dwight, A. E., U. S. At. Energy Comm. ANL-6516, 259-260 (1961).
9. Compton, V. B., and Matthias, B. T., Acta Cryst., 12, 651-654 (1959).
10. Dwight, A. E., U. S. At. Energy Comm. ANL-6330, 156-158 (1960).

TABLE 1

BINARY RARE EARTH-TRANSITION METAL ALLOYS IDENTIFIED AS LAVES PHASES

Alloy	Experimental Technique*	Lattice Parameters, A This Study a_o	 c_o	 Other Investigators a_o	 c_o	 Ref.
		Compositions of fcc $MgCu_2$ Type				
$EuIr_2$	LPS	7.566				
$EuPt_2$	LPS	7.731				
$TbIr_2$	ARC	7.532				
$TbPt_2$	ARC	7.618				
$DyIr_2$	ARC	7.517				
$DyPt_2$	ARC	7.602		7.5966		(7)
$HoPt_2$	ARC	7.591				
$ErPt_2$	ARC	7.570				
$YbCo_2$	LPS	7.115				
$YbRh_2$	LPS	7.432				
$YbIr_2$	LPS	7.477				
$LuFe_2$	ARC	7.217		7.222		(8)
$LuCo_2$	ARC	7.082				
$LuNi_2$	ARC	7.064		7.085		(8)
$LuRh_2$	ARC	7.422		7.412		(8)
$LuIr_2$	ARC	7.462				
		Compositions of Hexagonal $MgZn_2$ Type				
$PrOs_2$	LPS	5.370	8.960	5.368±2	8.945±2	(9)
$NdMn_2$	ARC					
$NdRe_2$	LPS	5.852	9.875			
$SmRe_2$	LPS					
$EuRe_2$	LPS	5.028	8.987			
$GdRe_2$	LPS	5.455	8.842			

TABLE 1 (Continued)

		Lattice Parameters, A				
		This Study		Other Investigators		
Alloy	Experimental Technique*	a_o	c_o	a_o	c_o	Ref.
$TbRu_2$	LPS	5.254	8.831			
$TbRe_2$	LPS	5.274	8.646			
$TbOs_2$	ARC	5.319	8.826			
$DyRu_2$	ARC	5.265	8.852	5.255	8.844	(10)
$DyRe_2$	ARC	5.391	8.804			
$DyOs_2$	ARC	5.307	8.792			
$HoRu_2$	ARC	5.263	8.827	5.244	8.8099	(10)
$HoRe_2$	ARC					
$HoOs_2$	ARC	5.295	8.772			
$ErRe_2$	ARC	5.375	8.767			
$ErOs_2$	ARC	5.291	8.755			
$TmRu_2$	LPS	5.246	8.790			
$TmRe_2$	LPS	5.187	9.070			
$TmOs_2$	LPS					
$YbRu_2$	LPS	5.211	8.744			
$YbRe_2$	LPS	5.340	8.685			
$YbOs_2$	LPS	5.244	8.626			
$LuMn_2$	ARC	5.203	8.517	5.228	8.590	(10)
$LuRe_2$	ARC	5.317	8.723	5.335	8.717	(10)

* ARC - arc-melted, LPS - liquid-phase sintered.

TABLE 2

BINARY RARE EARTH-TRANSITION METAL ALLOYS IDENTIFIED AS NEITHER $MgCu_2$ NOR $MgZn_2$ STRUCTURE

Alloy	Experimental Technique*	Remarks
No Intermetallic Compounds Found		
$LaRe_2$	LPS	La + Re + 5 unidentified lines
$CeRe_2$	LPS	Ce + Re
$PrRe_2$	LPS	Pr + Re
DyW_2	ARC	Dy + W--samples appeared sintered rather than completely melted.
$ErMo_2$	ARC	Er + Mo
$LuMo_2$	ARC	Lu + Mo
Other Intermetallic Compounds Present		
$TbPd_2$	ARC	Same structures(s), not identified.
$DyPd_2$	ARC	
$HoPd_2$	ARC	
$ErPd_2$	ARC	
$LuPd_2$	ARC	fcc pattern, $a_o = 4.02$ A, and unidentified lines.
$LuPt_2$	ARC	fcc pattern, $a_o = 4.02$ A, and unidentified lines.

---

* ARC - arc-melted, LPS - liquid-phase sintered.

TABLE 3

TERNARY RARE EARTH-TRANSITION METAL ALLOYS INVESTIGATED

Alloy	Experimental Technique*	Lattice Parameters, A			Other Phases
		$MgCu_2$ Type, a_o	$MgZn_2$ Type a_o	$MgZn_2$ Type c_o	
		$(Er + Sm)Mn_2$ System			
$SmMn_2$			Unknown		
$(0.2Er + 0.8Sm)Mn_2$	ARC	7.698			
$(0.4Er + 0.6Sm)Mn_2$	ARC	7.633			
$(0.6Er + 0.4Sm)Mn_2$	ARC	7.611			
$(0.8Er + 0.2Sm)Mn_2$	ARC		5.329	8.704	
$ErMn_2^{\dagger}$			5.281	8.621	
		$(Er + Gd)Mn_2$ System			
$GdMn_2^{\dagger}$		7.732			
$(0.2Er + 0.8Gd)Mn_2$	ARC	7.710			
$(0.4Er + 0.6Gd)Mn_2$	ARC	7.633			
$(0.6Er + 0.4Gd)Mn_2$	ARC	7.586			
$(0.8Er + 0.2Gd)Mn_2$	ARC		5.327	8.701	
$ErMn_2^{\dagger}$			5.281	8.621	
		$(Dy + Er)Mn_2$ System			
$DyMn_2^{\dagger}$		7.573			
$(0.8Dy + 0.2Er)Mn_2$	ARC	7.569			
$(0.6Dy + 0.4Er)Mn_2$	ARC	7.549			
$(0.5Dy + 0.5Er)Mn_2$	ARC		5.312	8.656	
$(0.4Dy + 0.6Er)Mn_2$	ARC		5.310	8.687	
$(0.2Dy + 0.8Er)Mn_2$	ARC		5.243	8.616	
$ErMn_2^{\dagger}$			5.281	8.621	

TABLE 3 (Continued

Alloy	Experimental Technique*	Lattice Parameters, A: $MgCu_2$ Type, a_o	Lattice Parameters, A: $MgZn_2$ Type a_o	Lattice Parameters, A: $MgZn_2$ Type c_o	Other Phases
		$(Er + Ho)Mn_2$ System			
$HoMn_2$†		7.507 ± 0.005			
$(0.9Ho + 0.1Er)Mn_2$	ARC		5.324	8.698	
$(0.8Ho + 0.2Er)Mn_2$	ARC		5.318	8.684	
$(0.6Ho + 0.4Er)Mn_2$	ARC		5.332	8.644	
$(0.4Ho + 0.6Er)Mn_2$	ARC		5.302	8.655	
$(0.2Ho + 0.8Er)Mn_2$	ARC		5.298	8.651	
$ErMn_2$†			5.281	8.621	
		$(Dy + Tm)Mn_2$ System			
$DyMn_2$†		7.5731			
$(0.8Dy + 0.2Tm)Mn_2$	ARC	7.561			
$(0.6Dy + 0.4Tm)Mn_2$	ARC		5.325	8.685	
$(0.4Dy + 0.6Tm)Mn_2$	ARC		5.298	8.676	
$(0.2Dy + 0.8Tm)Mn_2$	ARC		5.293	8.630	
$TmMn_2$†			5.241	8.565	
		$(Ho + Tm)Mn_2$ System			
$HoMn_2$†		7.507 ±0.005			
$(0.9Ho + 0.1Tm)Mn_2$	ARC	7.522			
$(0.8Ho + 0.2Tm)Mn_2$	ARC		5.311	8.695	
$(0.6Ho + 0.4Tm)Mn_2$	ARC		5.292	8.615	
$(0.4Ho + 0.6Tm)Mn_2$	ARC		5.272	8.590	
$(0.2Ho + 0.8Tm)Mn_2$	ARC		5.282	8.623	
$TmMn_2$†			5.241	8.565	

TABLE 3 (Continued)

Alloy	Experimental Technique*	Lattice Parameters, A MgCu$_2$ Type, a$_o$	MgZn$_2$ Type a$_o$	 c$_o$	Other Phases
Er(Cr + Mn)$_2$ System					
$ErCr_2$†					Er + Cr
Er(0.8Cr + 0.2Mn)$_2$	ARC				Er + Cr
Er(0.6Cr + 0.4Mn)$_2$	ARC		5.261	8.598	Er + Cr
Er(0.4Cr + 0.6Mn)$_2$	ARC		5.266	8.631	
Er(0.2Cr + 0.8Mn)$_2$	ARC		5.166	8.436	
$ErMn_2$†			5.281	8.621	
Tm(Cr + Mn)$_2$ System					
$TmCr_2$					Tm + Cr (?)
Tm(0.8Cr + 0.2Mn)$_2$	ARC		5.295	8.585	Tm + Cr
Tm(0.6Cr + 0.4Mn)$_2$	ARC		5.300	8.675	Tm
Tm(0.4Cr + 0.6Mn)$_2$	ARC		5.262	8.590	Tm
Tm(0.2Cr + 0.8Mn)$_2$	ARC		5.232	8.520	
$TmMn_2$†			5.241	8.565	
Lu(Cr + Mn)$_2$ System					
$LuCr_2$					Lu + Cr (?)
Lu(0.8Cr + 0.2Mn)$_2$	ARC		5.220	8.530	Lu + Cr
Lu(0.6Cr + 0.4Mn)$_2$	ARC		5.103	9.066	Lu + Mn
Lu(0.4Cr + 0.6Mn)$_2$	ARC		5.219	8.511	Lu + Mn
Lu(0.2Cr + 0.8Mn)$_2$	ARC		5.235	8.535	Lu + Mn
$LuMn_2$	ARC		5.203	8.517	

TABLE 3 (Continued)

Alloy	Experimental Technique*	Lattice Parameters, A MgCu$_2$ Type, a$_o$	MgZn$_2$ Type a$_o$	 c$_o$	Other Phases
		Er(Mn + Fe)$_2$ System			
ErMn$_2$†			5.281	8.621	
Er(0.8Mn + 0.2Fe)$_2$	ARC		5.255	8.596	
Er(0.7Mn + 0.3Fe)$_2$	ARC	7.425			
Er(0.6Mn + 0.4Fe)$_2$	ARC	7.398			
Er(0.4Mn + 0.6Fe)$_2$	ARC	7.353			
Er(0.2Mn + 0.8Fe)$_2$	ARC	7.314			
ErFe$_2$†		7.273 ±0.005			
		Tm(Mn + Fe)$_2$ System			
TmMn$_2$†			5.241	8.565	
Tm(0.8Mn + 0.2Fe)$_2$	ARC		5.229	8.584	
Tm(0.6Mn + 0.4Fe)$_2$	ARC	7.348	5.172	8.466	
Tm(0.4Mn + 0.6Fe)$_2$	ARC	7.041			
Tm(0.2Mn + 0.8Fe)$_2$	ARC	7.279			
TmFe$_2$†		7.247			
		(La + Nd)Os$_2$ System			
LaOs$_2$†		7.737 ±0.001			
(0.8La + 0.2Nd)Os$_2$	LPS	7.801	5.391	8.913	
(0.6La + 0.4Nd)Os$_2$	LPS		5.375	8.983	
(0.4La + 0.6Nd)Os$_2$	LPS		5.429	8.890	
(0.2La + 0.8Nd)Os$_2$	LPS		5.366	8.966	
NdOs$_2$†			5.368 ±0.002	8.926 ±0.001	

TABLE 3 (Continued)

Alloy	Experimental Technique*	Lattice Parameters, A			Other Phases
		MgCu$_2$ Type, a$_o$	MgZn$_2$ Type a$_o$	MgZn$_2$ Type c$_o$	
		(La + Gd)Os$_2$ System			
LaOs$_2$†		7.737 ±0.001			
(0.8La + 0.2Gd)Os$_2$	LPS	7.741	5.328	8.694	
(0.4La + 0.6Gd)Os$_2$	LPS		5.327	8.838	
(0.2La + 0.8Gd)Os$_2$	LPS		5.336	8.860	
GdOs$_2$†			5.319 ±0.002	8.838 ±0.002	
		(Ce + Gd)Os$_2$ System			
CeOs$_2$†		7.593 ±0.001			
(0.8Ce + 0.2Gd)Os$_2$	LPS		5.330	8.847	
(0.6Ce + 0.4Gd)Os$_2$	LPS		5.333	8.825	
(0.4Ce + 0.6Gd)Os$_2$	LPS		5.324	8.837	
(0.2Ce + 0.8Gd)Os$_2$	LPS		5.335	8.860	
GdOs$_2$†			5.319 ±0.002	8.838 ±0.002	
		(Sm + Gd)Ru$_2$ System			
SmRu$_2$†		7.580			
(0.8Sm + 0.2Gd)Ru$_2$	LPS	7.577	5.292	8.865	
(0.6Sm + 0.4Gd)Ru$_2$	LPS		5.280	8.922	
(0.4Sm + 0.6Gd)Ru$_2$	LPS		5.283	8.914	
(0.2Sm + 0.8Gd)Ru$_2$	LPS		5.298	8.927	
GdRu$_2$†			5.271 ±0.002	8.904 ±0.002	

* ARC - arc-melted, LPS - liquid-phase sintered.

† Parameter values taken from literature.

FIGURE TITLES

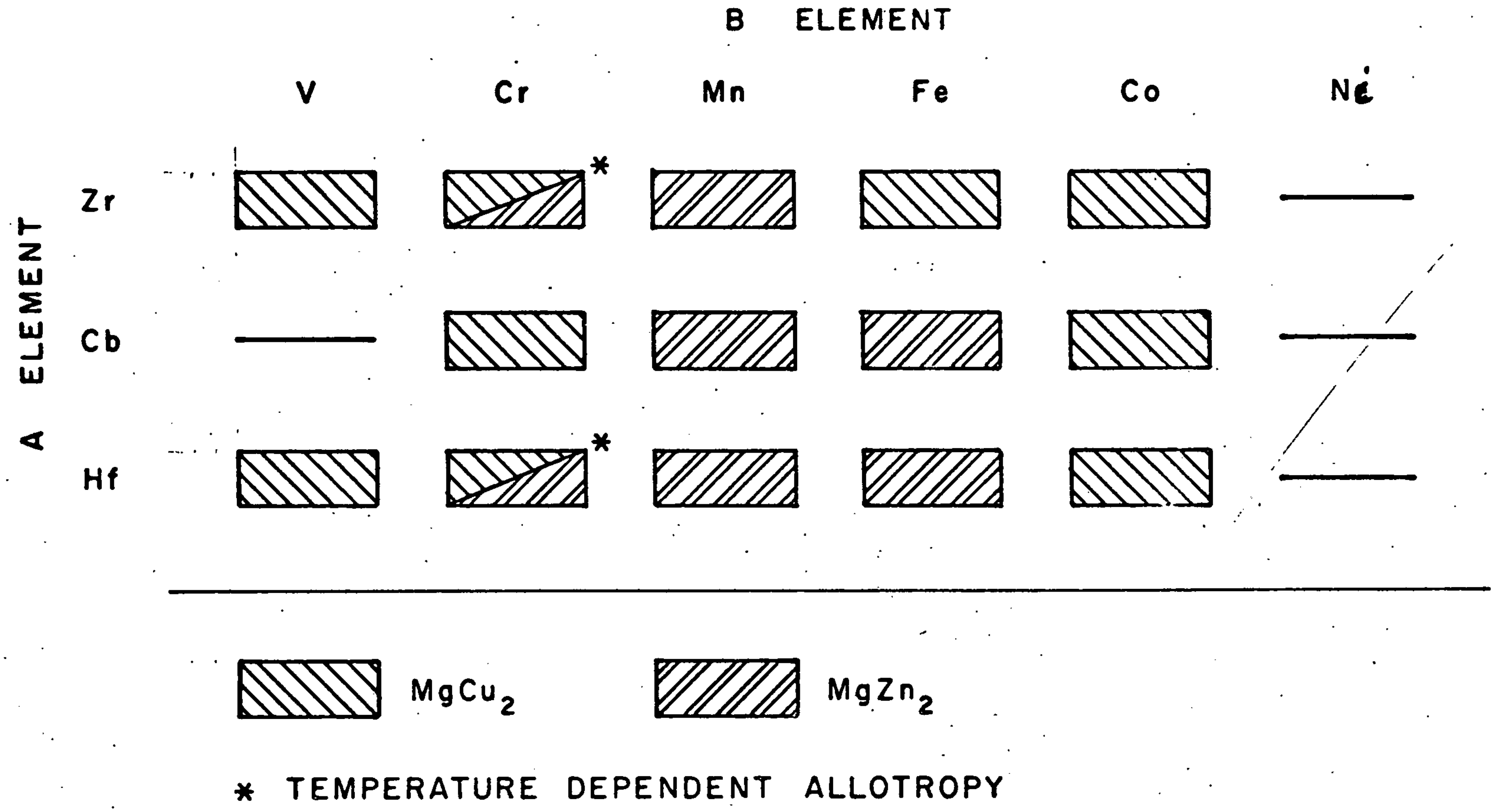

FIG. 1 - Crystal Structures of Transition Metal-Transition Metal Laves Phases

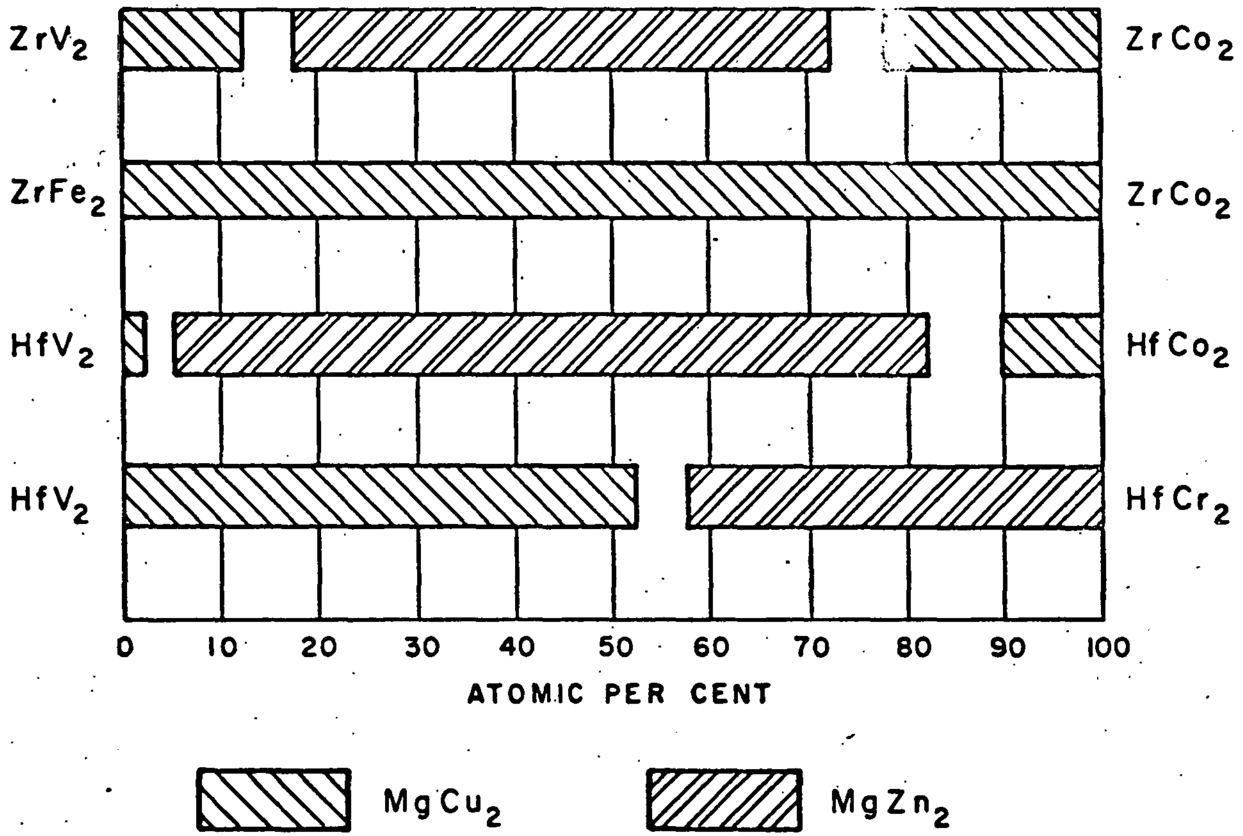

FIG. 2 - Ternary Miscibility Between Transition Metal-Transition Metal Laves Phases.

B – ELEMENT

A – ELEMENT	IVa	Va	VIa	VIIa	VIIIa	VIIIb	VIIIc
	Ti	V	Cr	Mn	Fe	Co	Ni
Sc	NC 1.12*	X 1.21	NC 1.28	▨ 1.20	▨ 1.27	▧ 1.30	▧ 1.31
Y	NC 1.22	NC 1.32	NC 1.41	▧ 1.31	▧ 1.40	▧ 1.43	▧ 1.44
La	NC 1.28	NC 1.38	NC 1.47	NC 1.37	NC 1.46	X 1.49	▧ 1.50
Ce	NC 1.24	NC 1.35	NC 1.43	NC 1.34	▧ 1.42	▧ 1.45	▧ 1.46
Pr	X 1.24	NC 1.35	X 1.43	X 1.34	X 1.42	▧ 1.45	▧ 1.46
Nd	NC 1.24	NC 1.34	X 1.42	▨ 1.33	X	▧ 1.44	▧ 1.46
Pm	X 1.23	X 1.33	X 1.41	X 1.39	X 1.42	X 1.44	X 1.44
Sm	X 1.22	X 1.32	X 1.41	X 1.31	▧ 1.40	▧ 1.43	▧ 1.44
Eu	X 1.39	X 1.50	X 1.59	X 1.49	X 1.58	X 1.62	X 1.63
Gd	NC 1.22	NC 1.32	NC 1.41	▧ 1.31	▧ 1.40	▧ 1.43	▧ 1.44
Tb	X 1.21	X 1.31	X 1.39	▧ 1.30	X 1.38	▧ 1.41	▧ 1.42
Dy	NC 1.20	NC 1.30	NC 1.38	▧ 1.29	▧ 1.37	▧ 1.40	▧ 1.42
Ho	X 1.20	X 1.30	NC 1.38	▧ 1.29	▧ 1.37	▧ 1.40	▧ 1.42
Er	NC 1.20	X 1.29	NC 1.38	▨ 1.28	▧ 1.36	▧ 1.40	▧ 1.41
Tm	X 1.19	X 1.29	X 1.37	▨ 1.28	▧ 1.36	▧ 1.39	X 1.40
Yb	X 1.32	X 1.43	X 1.52	X 1.42	X 1.50	▧ 1.54	▧ 1.55
Lu	X 1.18	NC 1.27	X 1.35	▨ 1.26	▧ 1.34	▧ 1.37	▧ 1.38

KEY: ▨ $MgZn_2$ ▧ $MgCu_2$

$* \frac{dA}{dB}$ X, UNKNOWN NC, NO COMPOUNDS

FIG. 3 - Crystal Structures of Laves Phases Formed Between the Rare Earth Elements and Metals of the First Transition Series.

B — ELEMENT

A – ELEMENT	IV a Zr	V a Cb	VI a Mo	VII a (Tc)	VIII a Ru	VIII b Rh	VIII c Pd
Sc	X 1.01*	X 1.12	X 1.17	▨	▨ 1.24	X 1.21	X 1.19
Y	NC 1.11	NC 1.22	NC 1.29		▨ 1.36	▧ 1.33	X 1.30
La	NC 1.16	NC 1.28	NC 1.34		▧ 1.42	▧ 1.39	X 1.36
Ce	NC 1.13	NC 1.24	NC 1.31		▧ 1.39	▧ 1.36	X 1.33
Pr	X 1.13	X 1.24	X 1.31		▧ 1.39	▧ 1.36	X 1.33
Nd	X 1.12	X 1.24	X 1.30		▧ 1.38	▧ 1.35	X 1.32
Pm	X 1.13	X 1.23	X 1.29		X 1.35	X 1.35	X 1.32
Sm	X 1.11	X 1.22	X 1.29		▧ 1.36	X 1.33	X 1.30
Eu	X 1.26	X 1.39	X 1.46		X 1.55	X 1.51	X 1.48
Gd	NC 1.11	NC 1.22	NC 1.29		▨ 1.36	▧ 1.33	X 1.30
Tb	X 1.10	X 1.21	X 1.34		▨ 1.35	X 1.32	X 1.29
Dy	NC 1.09	NC 1.20	NC 1.26		▨ 1.34	▧ 1.31	X 1.28
Ho	X 1.09	X 1.20	X 1.26		▨ 1.34	▧ 1.31	X 1.28
Er	NC 1.09	X 1.20	NC 1.25		▨ 1.34	▧ 1.30	X 1.28
Tm	X 1.08	X 1.19	X 1.25		X 1.33	X 1.30	X 1.27
Yb	X 1.20	X 1.32	X 1.39		▨ 1.47	▧ 1.44	X 1.41
Lu	X 1.07	X 1.18	X 1.24		▨ 1.31	▧ 1.28	X 1.25

KEY: ▨ $MgZn_2$ ▧ $MgCu_2$

$*\frac{dA}{dB}$ X, UNKNOWN NC, NO COMPOUNDS

FIG. 4 - Crystal Structures of Laves Phases Formed Between the Rare Earth Elements and Metals of the Second Transition Series.

B - ELEMENT

A - ELEMENT	IVa Hf	Va Ta	VIa W	VIIa Re	VIIIa Os	VIIIb Ir	VIIIc Pt
Sc	X 1.03*	NC 1.12	X 1.16	▨ 1.20	▨ 1.22	▧ 1.21	X 1.18
Y	NC 1.13	NC 1.22	NC 1.28	▨ 1.31	▨ 1.33	▧ 1.32	▧ 1.29
La	X 1.18	NC 1.28	X 1.33	NC 1.37	▧ 1.39	▧ 1.38	▧ 1.35
Ce	X 1.14	NC 1.24	X 1.30	NC 1.34	▧ 1.36	▧ 1.35	▧ 1.32
Pr	X 1.14	NC 1.24	X 1.30	NC 1.34	▨ 1.36	▧ 1.35	▧ 1.32
Nd	X 1.14	NC 1.24	X 1.29	▨ 1.33	▨ 1.35	▧ 1.34	▧ 1.31
Pm	X 1.13	X 1.23	X 1.28	X 1.32	X 1.34	X 1.33	X 1.30
Sm	X 1.13	NC 1.22	X 1.28	▨ 1.31	▨ 1.33	X 1.32	X 1.29
Eu	X 1.28	NC 1.39	X 1.45	▨ 1.49	X 1.51	▧ 1.50	▧ 1.47
Gd	X 1.12	NC 1.22	NC 1.28	▨ 1.31	▨ 1.33	▧ 1.32	▧ 1.29
Tb	X 1.11	NC 1.21	X 1.26	▨ 1.30	▨ 1.32	▧ 1.31	▧ 1.28
Dy	X 1.11	NC 1.20	X 1.26	▨ 1.29	▨ 1.31	▧ 1.30	▧ 1.27
Ho	X 1.11	NC 1.20	X 1.26	▨ 1.29	▨ 1.31	▧ 1.30	▧ 1.27
Er	X 1.10	NC 1.20	X 1.25	▨ 1.28	▨ 1.30	▧ 1.29	▧ 1.27
Tm	X 1.09	NC 1.19	X 1.24	▨ 1.28	▨ 1.30	X 1.29	X 1.26
Yb	X 1.21	NC 1.32	X 1.38	▨ 1.42	▨ 1.44	▧ 1.43	X 1.40
Lu	X 1.08	NC 1.17	X 1.23	▨ 1.26	▨ 1.28	▧ 1.27	X 1.24

KEY: ▨ $MgZn_2$ ▧ $MgCu_2$

$* \frac{dA}{dB}$ X, UNKNOWN NC, NO COMPOUNDS

FIG. 5 - Crystal Structures of Laves Phases Formed Between the Rare Earth Elements and Metals of the Third Transition Series

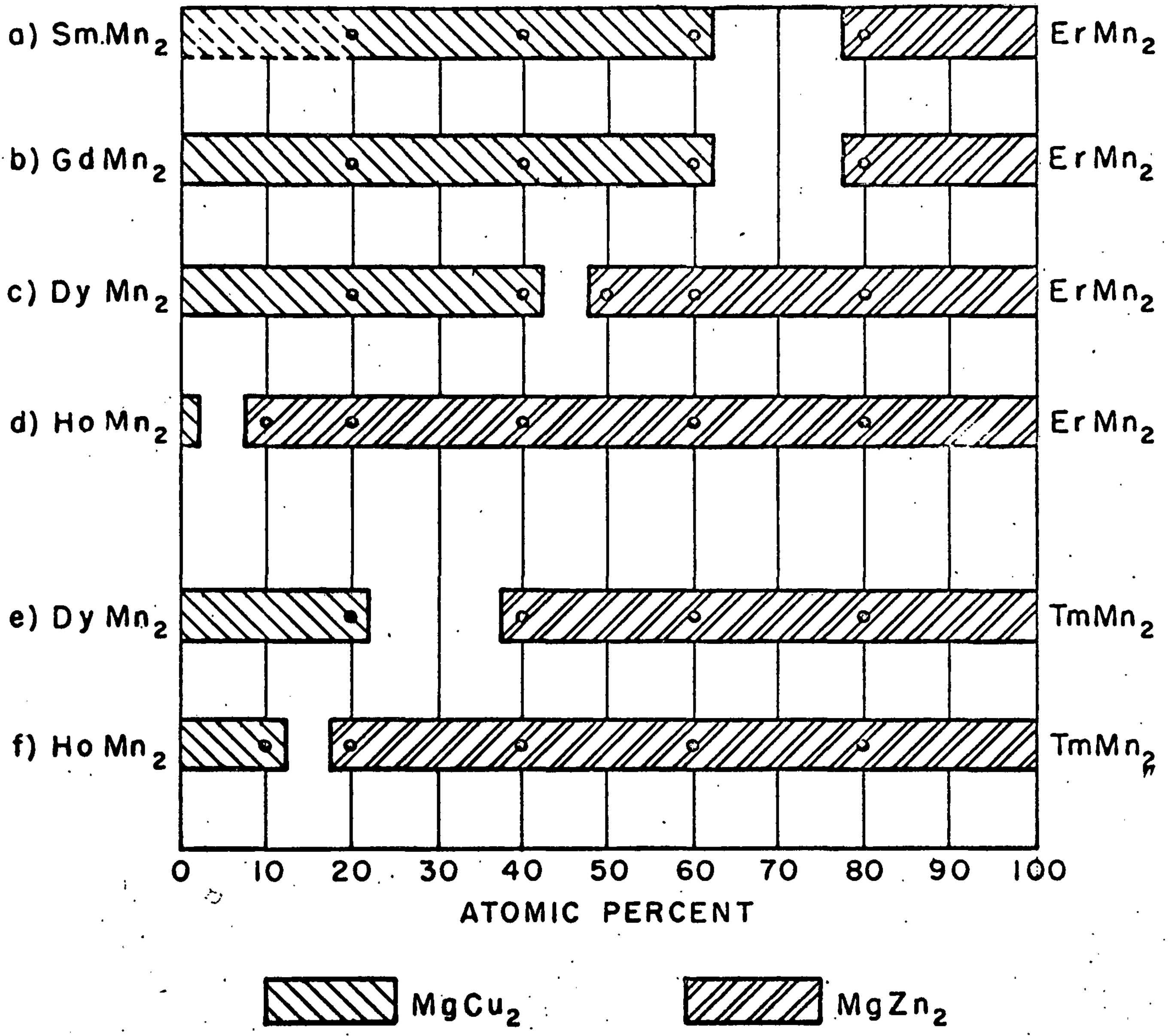

FIG. 6 - Ternary Miscibility of Rare Earth Element-Transition Metal Laves Phases, I.

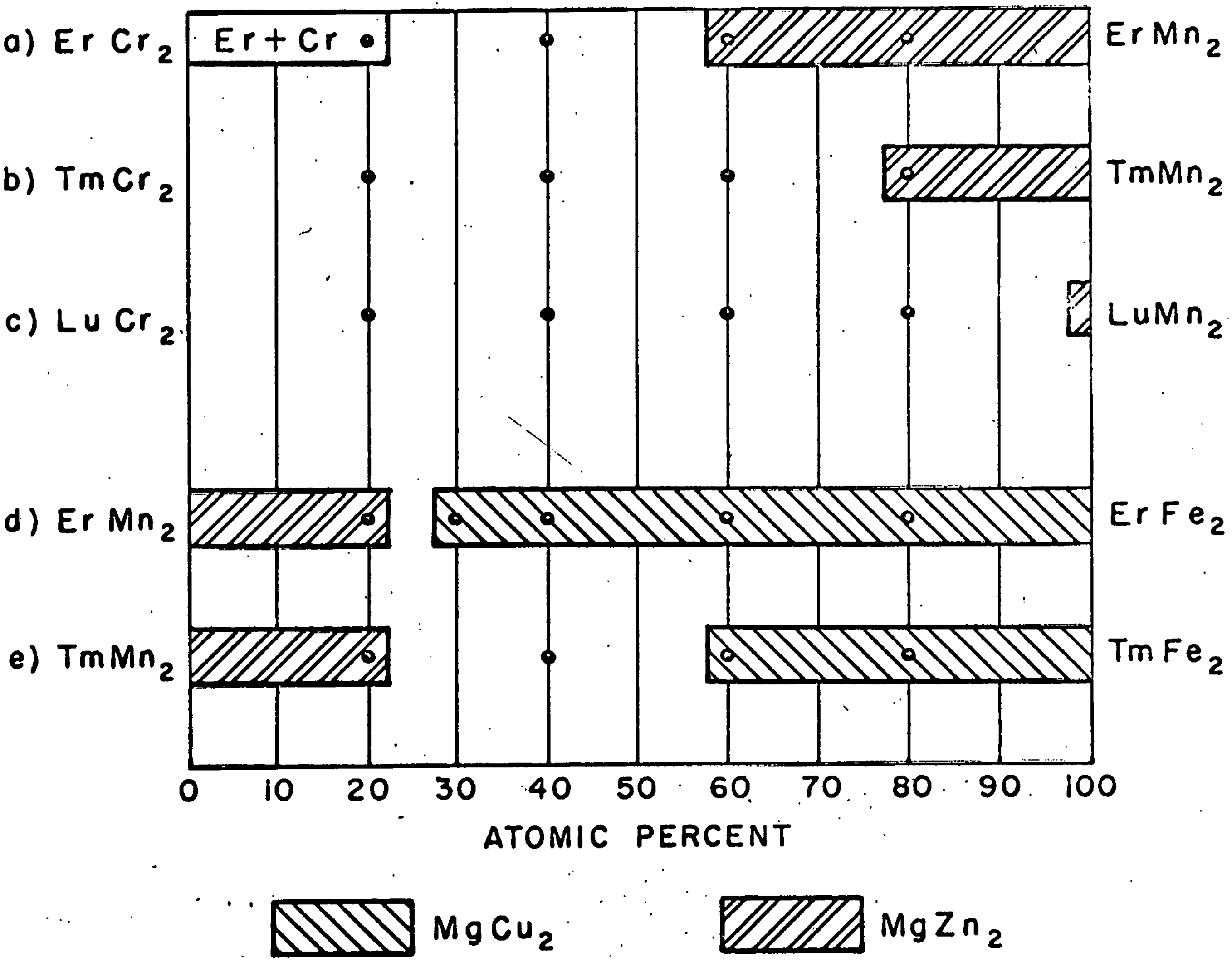

FIG. 7 - Ternary Miscibility of Rare Earth Element-Transition Metal Laves Phases, II.

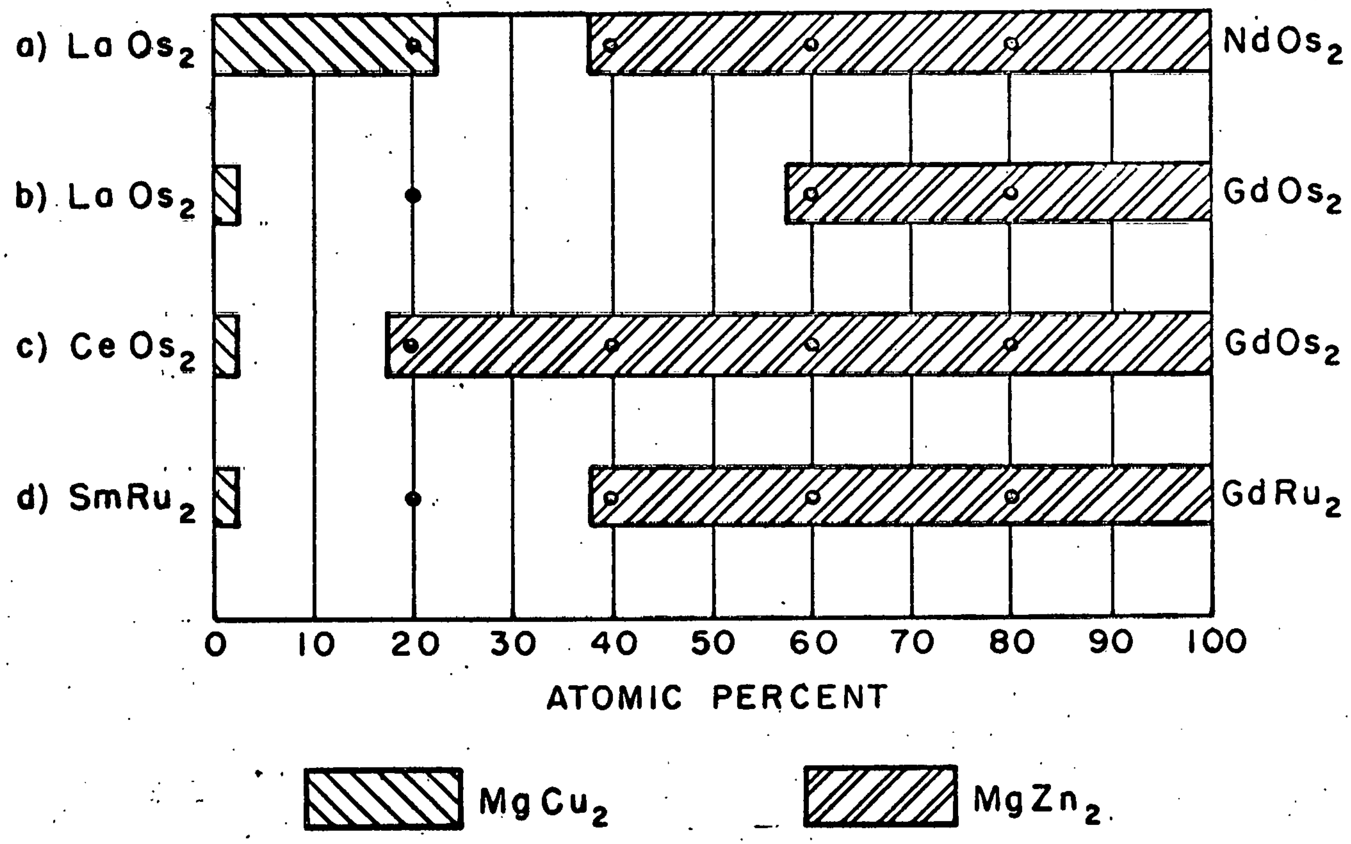

FIG. 8 - Ternary Miscibility of Rare Earth Element - Transition Metal Laves Phases, III

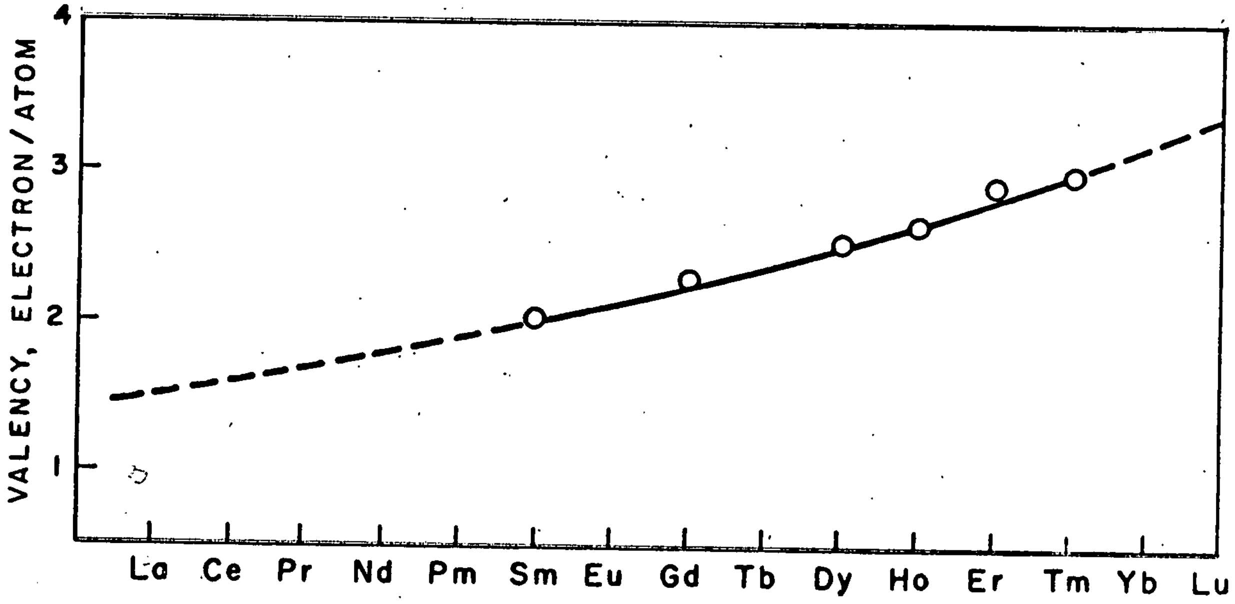

FIG. 9 - Valencies of the Rare Earth Elements.